

# Development of Holistic Climate Simulation Codes for a non-Hydrostatic Atmosphere-Ocean Coupled Systems

Project Representative

Keiko Takahashi The Earth Simulator Center

Author

Keiko Takahashi The Earth Simulator Center

In this report, we present preliminary validation results of the developed non-hydrostatic atmosphere and ocean components. We describe outline of model configuration and physical performance of the each component. We have performed experiments of 72 hours forecast with the global cloud permitting atmosphere model which has developed in the Earth Simulator Center and those physical performance shows comparable results compared observational data. In addition, typhoon tracking and intensity of precipitation for 72 hours forecast experiments have been showed and a part of results was presented in this report. 15 years integration of North Pacific basin has been carried out and reasonable performance has been obtained with the ocean component. Using nesting scheme, seasonal variability along east coast in Kanto region has been presented in order to confirm the physical performance of our ocean component.

**Keywords:** non-hydrostatic dynamical core, AGCM, OGCM, coupled atmosphere-ocean model, cloud micro physics, typhoon tracking

## 1. Introduction

In the Earth Simulator Center, we have been developing a global/regional coupled non-hydrostatic atmosphere-ocean-land simulation code with high computational performance since FY2003. This simulation code was designed for the purpose of research multi-scale or multi-physics phenomena in coupled atmosphere – ocean system. The simulation code will bring us useful tools to research simultaneously global climate and regional weather/climate and interactions between weather and phenomena with synoptic scale.

In this report, validation results of the global/regional non-hydrostatic atmosphere/ocean simulation code, which is designed and built from scratch in the Earth Simulator Center, are mainly presented. Configuration of the coupled simulation code, which is characterized by a grid system, high order discretization schemes, interpolation schemes and coupling schemes, is described in section 2. In section 3, we present results of several experiments with micro-cloud physics. Furthermore, results of typhoon tracking prediction trials are presented. In section 4, brief summary and near future work conclude this report.

## 2. Model configuration

### 2.1 Grid system

Yin-Yang grid system[1], which was developed by Dr. Kageyama of Solid Earth Simulation Group in the Earth Simulator Center, is used to atmosphere, land and ocean

components. By having this new grid system, we can avoid the problem of how to cover singular points such as the south and north poles. The advantage to enlarge the time step makes progresses of computational performance to be compared with conventionally utilized latitude/longitude grid systems.

### 2.2 Governing equations and discretization

In the atmospheric component, fully compressive three-dimensional Navier-Stokes equations with rotational effects (1), continuity equation (2), pressure equation (3) and the equation of the state (4) are used as follows[2]. Forecast variables are perturbation density, three components of momentum, and perturbation pressure.

$$\frac{\partial \rho \mathbf{v}}{\partial t} + \nabla p' + \rho' \mathbf{g} = -\nabla \cdot (\rho \mathbf{v} \mathbf{v}) + 2 \rho \mathbf{v} \times \mathbf{f} + \mu (\nabla^2 \mathbf{v} + \frac{1}{3} \nabla \cdot (\nabla \mathbf{v})) \quad (1)$$

$$\frac{\partial \rho'}{\partial t} + \nabla \cdot (\rho \mathbf{v}) = 0 \quad (2)$$

$$\frac{\partial P'}{\partial t} + \bar{\rho} \mathbf{g} w + \mathbf{v} \nabla P' + \gamma P \nabla \mathbf{v} = (\gamma - 1) \kappa \nabla^2 T + (\gamma - 1) \Phi \quad (3)$$

$$P = \rho RT \quad (4)$$

The treatment of cloud and precipitation is controlled by

selecting one of parameterization schemes due to horizontal resolution. For grid spacing greater than 10 km, Kain and Fritsch scheme is used and cloud micro physics based on mixed phase micro cloud physics [3] is used for below 5 km horizontal spacing. Over land, the ground temperature and ground moisture are computed by using a bucket model as a simplified land model. As upper boundary condition, Rayleigh friction layer is set. For the lateral boundary condition of regional model version, sponge type boundary condition [4] is used.

In the ocean component, at present stage, incompressible and hydrostatic non-hydrostatic equations with the Boussinesq approximation are used based on describing in [5][6]. As an additional formulation, UNESCO scheme [7] is used in order to obtain density in the ocean.

Arakawa-C grid for horizontal spacing is used in both components. Height-based terrain-following in the atmospheric component and z-coordinate in the ocean component are introduced for vertical discretization. Lorenz type vertical representation of parameters is used for both components.

Several discretization schemes are available to be selected. Especially, it is confirmed that 5<sup>th</sup> order upwind finite difference method for advection terms and 4<sup>th</sup> order flux form of other terms by central differencing are stable with high accuracy. The 2<sup>nd</sup>, 3<sup>rd</sup> and 4<sup>th</sup> order Runge-Kutta schemes for large time-step integration and forward-backward scheme for small time-step integration are used in the atmospheric component. In the ocean component, leap-frog scheme with Robert-Asselin time filter is also adopted. 2<sup>nd</sup> order horizontal/vertical numerical viscosity and divergence damping are introduced.

Further information of the model configuration is described in Table 1.

### 2.3 Sound wave

In atmospheric component, vertical speed of sound is usually dominant comparing with its of horizontal direction,

because vertical resolution is tend to be finer than horizontal discretization. Therefore, we use horizontally explicit vertical implicit (HEVI) scheme [8] in the atmosphere component.

Since a speed of sound wave in the ocean is three times faster than it in the atmosphere, implicit method to solve Poisson equation (5) such that

$$\nabla \cdot \text{grad}P' = B \quad (5)$$

where

$$B = \rho_0 \nabla \cdot \mathbf{G}_v = \frac{\rho_0}{r \cos \varphi} \frac{\partial}{\partial \lambda} G_u + \frac{\rho_0}{r \cos \varphi} \frac{\partial}{\partial \varphi} (\cos \varphi G_v) + \frac{\rho_0}{r^2} \frac{\partial}{\partial r} (r^2 G_w), \quad (6)$$

is adopted under Neumann boundary condition which is defined as  $n \cdot \text{grad}P = n \cdot \mathbf{G}_v$ .

Furthermore, Algebraic Multi-Grid (AMG) method [9] is introduced in order to solve Poisson equation (5), which is well known as an optimal solution method. In fact, we used AMG library which has been developed by Fuji Research Institute Corporation. In the library, AMG method is developed based on aggregation-type AMG and is used as a preconditioner in Kiylov subspace algorithms. Incomplete LU decomposition (ILU) is adopted as a smoother, which can show good computational performance even for ill-structured matrixes.

### 2.4 Boundary interface between Yin-Yang grid panels

Boundary conditions between grid panels in Yin-Yang grid system is specified for the velocity and scalar fields using 6<sup>th</sup> order Lagrange polynomials interpolation. One of essential issues on overset grid systems such as Yin-Yang grid system is a conservation problem. We have introduced a mass imbalance correction scheme on a boundary of each panels, which was introduced in [10][11]. We have confirmed that time evolution of relative error by using the introduced mass conserva-

Table 1 Outline of the atmosphere/ocean model configuration.

		Non-hydrostatic AGCM	Non-hydrostatic OGCM
Equations System		Fully compressive N-S equations	non-hydrostatic incompressive N-S equations
Grid System		Yin-Yang grid system	Yin-Yang grid system
Discrimination	Space	Arakawa-C grid (horizontal), z* (vertical)	Arakawa-C grid (horizontal), z (vertical)
	Time	4th order Runge-Kutta	4th order Runge-Kutta
Advection terms		5th order flux form, CIP-OSLR	5th order flux form
not Advection terms		4th order flux form	4th order flux form
Sound wave		HEVI, HIVI	Implicit methods (2-dimensional, 3-dimensional)
Gravity wave		-	-
Microphysics		Qc, Qci, Qr, Qs, Qg	-
Cumulus Param.		Kain-Fritsch scheme	-
Turbulence		Smagorinsky scheme (static), dynamic Smagorinsky [LES]	Smagorinsky scheme (static), dynamic Smagorinsky [LES]
		Nesting schemes (1 way, 2 way)	Nesting schemes (1 way, 2 way)
			Tide, Multi-grid Methods (Poisson equations)
Parallelization		2-dim. decomposition, inter nodes:MPI, intra nodes:micro-task	2-dim. decomposition, inter nodes:MPI, intra nodes:micro-task

tion scheme changes within the limit of rounding error.

### 2.5 Grid-nesting scheme

The grid-nesting scheme is also introduced not only to atmosphere but ocean components. Improving model resolution, meso-scale phenomena in a focused region should be represented clearly. In addition of conventional widely used one-way nesting scheme, online one-way scheme on the Earth Simulator, which is able to handle global and regional model experiments at the same time, is introduced with high computational performance.

## 3. Validation experiments and results

### 3.1 Performance of the atmospheric component

Results of several benchmark test experiments suggest that no “side-effects” on overlapped grids in Yin-Yang grid system are shown in [12][13][14]. In fact, Williamson’s tests experiments for shallow water equations, three dimensional mountain waves and Held-Suarez experiments of 1000 days integration have been performed. Those results have shown being comparable with results of previous studies. [12][13][14].

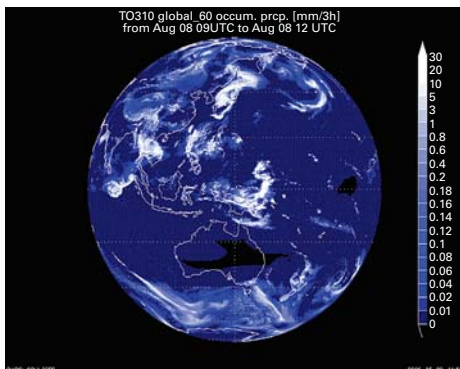
In addition to experiments of dynamical core, global simulation to validate physical performance has been performed under the condition of 11 km / 5.5 km horizontal resolution with 32 vertical layers. In experiments, the atmosphere component includes only cloud micro-physics in spite of cumulus parameterization, although 11 km horizontal resolution is

not suitable to be a cloud resolving model. 72 hours integration was executed to validate physical performance. Initialized data was interpolated at 09:00 8<sup>th</sup> Aug2003 from Grid Point Value (GPV) data provided by Japan Meteorological Business Support Center. Sea surface data was also made by GPV data delivered form 09:00 7<sup>th</sup> to 09:00 8<sup>th</sup> Aug2003 and used cyclically during the simulation. Precipitation distribution for global is presented in Fig. 7(a). Precipitation distribution is corresponding to observational cloud distribution from the satellite GOES9 shown in Fig. 7(b).

Regional model validation has been performed with one way nesting from 5.5 km global simulation to 1.15 km horizontal with 64 vertical layers. Initialized data was also interpolated by using GPV data at 09:00 8<sup>th</sup> Aug2003. Boundary condition was made by interpolation from the above global simulation with 5.5 km horizontal resolution. Sea surface temperature was also used cyclically from 09:00 07<sup>th</sup> Aug to 09:00 8<sup>th</sup> Aug2003 during the simulation. 72-hours integration has been performed. Fig. 2 shows the result after 72 hours integration. Meso- $\gamma$  scale disturbance such as rain band might be captured in the simulations so that detail analysis is required.

### 3.2 The Ocean components validation

In stand alone ocean component, as validation simulations, 15-years integration with 11 km horizontal resolution and 40 vertical layers has been performed for the North Pacific basin. Surface heat fluxes and boundary data are computed from climatological data provided by World Ocean Atlas (WOA). Momentum fluxes are obtained by interpolating from climatological data by NCAR. Fig. 3 shows the snapshot in April after 15 years integration. Fig. 3 shows temperature distribution at 15 m depth from the sur-



(a) Simulation results of precipitation distribution during from 09UTC 08 Aug to 12UTC 08Aug.



(b) Observational data

Fig. 1 Global cloud permitting simulation with 5.5 km horizontal resolution (a) and observational data (b).

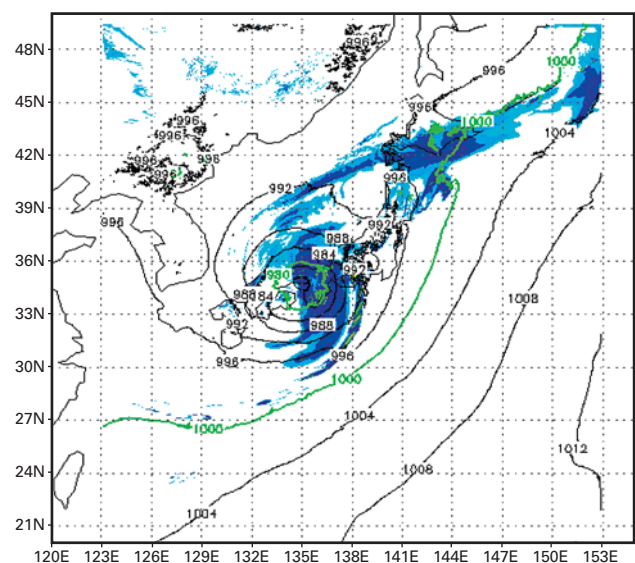
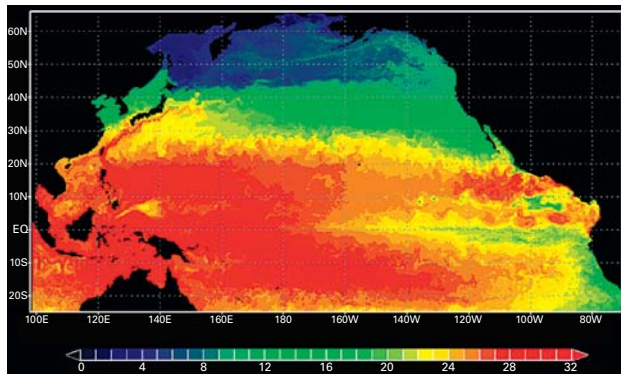


Fig. 2 Precipitation (mm/hour) and SLP distribution of ETAU.

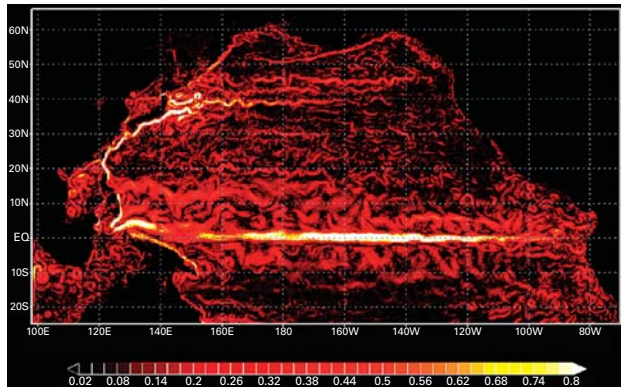


face, which is corresponding to the second layer from the surface. Fig. 3(b) shows distribution of absolute value of horizontal velocity at 105 m depth. Clear eddy resolved distributions have been recognized in both Fig. 3(a) and (b).

In the ocean component, regional validation has been also performed with one way nesting from North Pacific region with 11 km horizontal resolution simulation to Japanese Tokai-Kanto region with 2.27 km for horizontal and 40 vertical layers. Fig. 4 shows variation of sea surface temperature with the Kuroshio north going during winter-summer season. The seasonal basin-scale circulation in Tokyo bay

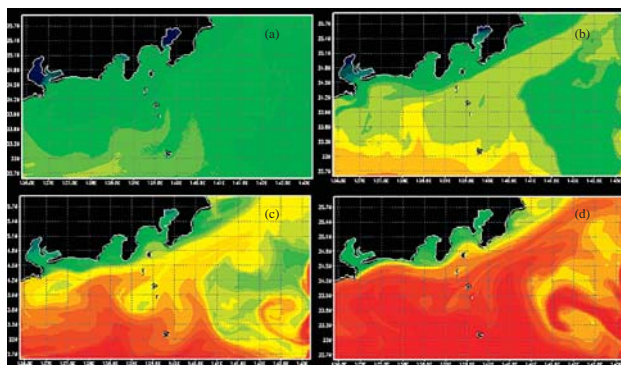


(a) Sea surface temperature distribution



(b) Velocity distribution at 105m depth

Fig. 3 Simulation results of North Pacific basin after 15 years integration.



(a)winter , (b) early spring , (c) spring, and (d) early summer

Fig. 4 Seasonal Simulation results of North Pacific basin after 15 years integration.

area has been influenced by the Kuroshio on progress of seasons.

### 3.3 Prediction experiments of typhoon tracking and its intensity

72 hours prediction experiments have been performed in order to show physical performance of the atmosphere component which is characterized by cloud permitted model as mentioned before. These 72 hours global forecast experiments initialized at 09:00 8<sup>th</sup> August 2003 have been performed with 11 km or 5.5 km horizontal resolution with 64 or 32 vertical layers respectively. In those forecast experiments, sea surface temperature changed from 09:00 8<sup>th</sup> August until 09:00 9<sup>th</sup> August was used cyclically as boundary data. In Fig. 5, tracking forecast of ETAU and the official 'best track' (presented in a black line) which is reported by Japan Meteorological Agency are shown. Simulated tracking in all cases are comparable to the best track, even if horizontal/vertical resolution has been changed.

After 72 hours prediction had been performed with 5.5 km resolved global atmosphere component, one way nested experiment with 1.15 km in Japanese region was executed. Fig. 6 presents precipitation distribution summed up during the term from 18:00 on 7<sup>th</sup> to 24:00 on 9<sup>th</sup> August in 2003 when ETAU attacked Japanese region. The distribution results simulated by global simulation with 5.5 km horizontal resolution are comparable to observed data as shown in Fig. 6(a) and (c). Simulation predicts two peaks of intensity in Kii peninsula, although amount of rain is lower than it of observational data. Fig. 6(b) shows precipitation distribution simulated by nesting scheme with 1.15 km horizontal resolution in Japanese region. It is clear that its intensity is different from those of 5.5 km/11 km global simulations. In fact, maximum intensity of wind is stronger in 1.15 km resolution simulations than simulations with 5.5 km/11 km horizontal resolution (data not shown). It might suggest that micro cloud physics and turbulent model in the atmosphere component works well under conditions with 1.15 km resolution.

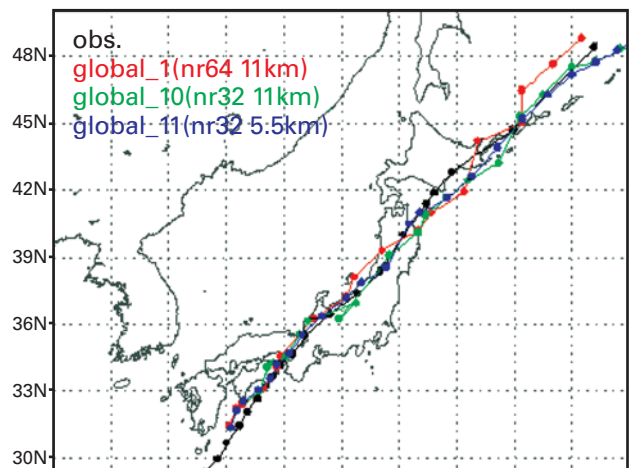
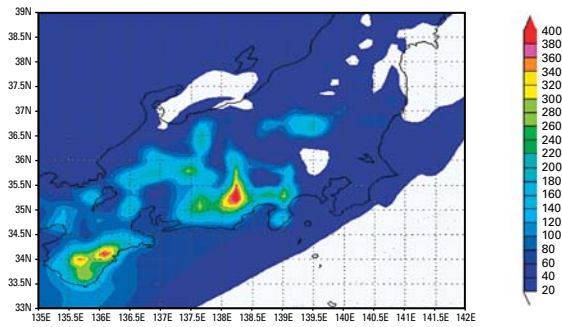
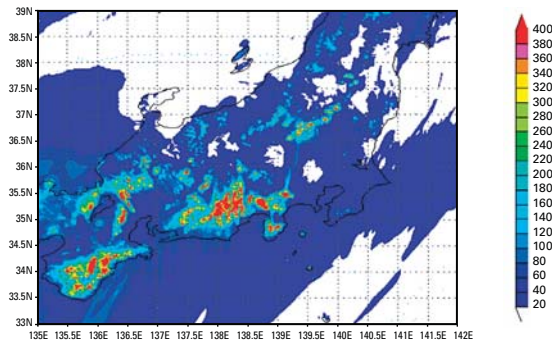


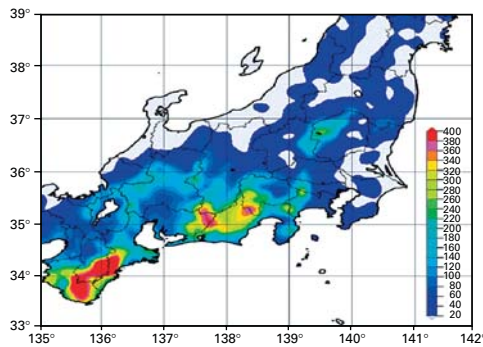
Fig. 5 72 hours tracking forecasting of Typhoon ETAU in 2003.



(a) Simulated results of precipitation with 5.5km horizontal resolution.



(b) Precipitation results in nested Japanese region with 1.15 km horizontal resolution



(c) Observation data from JMA.

Fig. 6 Precipitation from 0900 UTC 7th to 0300UTC 9<sup>th</sup> August in 2003.

Further analysis is still required to be clear those differences.

In the case of a global atmospheric component with 11 km horizontal resolution and 32 vertical levels, it takes about 14,000 seconds to finish 72 hours forecasting by using 48 nodes of the Earth Simulator. For the 5.5 km horizontal resolution, 72 hours forecasting took under 14,000 seconds using 192 nodes on the Earth Simulator.

#### 4. Near future work

In this report, preliminary validation results of both the atmospheric and ocean components were presented. Those results encourage us to further research/prediction of non-hydrostatic phenomena such as typhoon, heavy rain. The first step on development of both the atmospheric and the ocean components has been completed. Series of experiments using the non-hydrostatic coupled ocean-atmosphere model will be

started in the near future.

In addition, the following development will be pursued. First, optimization with a conservative semi-Lagrangian scheme with rational function (CIP-CSLR) [12], a chemical model and an urban models will be introduced, we are going to challenge target simulations for weekly, monthly, and seasonal prediction experiments with our non-hydrostatic coupled atmosphere-ocean model will be started.

#### References

- [1] A. Kageyama and T. Sato, *Geochem.Geophys.Geosyst.*, 5, Q09005, doi:10.1029/2004GC000734 (2004).
- [2] K. Takahashi, et al., *Proc. 7th International Conference on High Performance Computing and Grid in Asia Pacific Region*, 487 (2004).
- [3] Reisner, J., Ramussen R. J., and Bruintjes, R. T., Explicit forecasting of supercooled liquid water in winter storms using the MM5 mesoscale model. *Quart. J. Roy. Meteor. Soc.* (1998).
- [4] Davies, H. C., A lateral boundary formulation for multi-level prediction models, *Quart. J. R. Met. Soc.*, 102, 405-418 (1976).
- [5] Marshall, J., Hill, C., Perelman, et al., Hydrostatic, quasi-hydrostatic, and nonhydrostatic ocean modeling. *Journal of Geophysical Research*, 102, 5733-5752 (1997).
- [6] Marshall, J., Adcroft, A., et al., A finite-volume, incompressible Navier Stokes model for studies of the ocean on parallel computers. *Journal of Geophysical Research*, 102, 5753-5766 (1997).
- [7] A. Gill, *Atmosphere-Ocean dynamics*, Academic Press Inc., (1982).
- [8] Wicker, L. J., Skamarock, W.C., Time-splitting methods for elastic models using forward time schemes, *Monthly Weather Review*, 130, 2088-2097 (2002).
- [9] Klaus Stuben, "A Review of Algebraic Multigrid", GMD Report 96 (1999).
- [10] X. Peng, F. Xiao, et al, *QJR Meteorol Soc.* (submitted).
- [11] X. Peng, F. Xiao and K. Takahashi, The 2004 Workshop on the solution of partial differential equations on the sphere (2004).
- [12] K. Komine, K.Takahashi et al., The 2004 Workshop on the Solution of Partial Differential Equations on the Sphere (2004).
- [13] M. Ohdaira, K. Takahashi, et al. *Proc. of 2004 Workshop on the Solution of Partial Differential Equations on the Sphere*, (2004).
- [14] X. Peng, F. Xiao, K. Takahashi and T. Yabe, *JSME international Journal (Series B)*, 47(4), 725 (2004).
- [15] T.Sugimura, K.Takahashi et al. *Proc. of 2003 Autumn Meeting of the MSJ*, 351 (2003) (in Japanese)

# 地球シミュレータ用・非静力・大気海洋結合モデルの開発

プロジェクト責任者

高橋 桂子 地球シミュレータセンター

著者

高橋 桂子 地球シミュレータセンター

キーワード: non-hydrostatic dynamical core, AGCM, OGCM, coupled atmosphere-ocean model, cloud micro physics, typhoon tracking

地球シミュレータセンターでは、2003年度から非静力学・大気海洋結合モデルを開発しており、昨年度末までに、基本モデルの設計と開発、およびベンチマークテストによる初期性能検証を終了している。本年度は、新たな高精度数値計算スキームの導入、雲微物理モデルや放射過程、陸面過程、河川モデルなどの導入やそれらの改善と、新たな物理スキームの導入、さらに本結合モデルを構成する大気、海洋の各コンポーネントの物理的性能評価に焦点をあててモデル開発を進めてきた。

大気コンポーネントの物理的性能評価のための数値実験として、現実的な地形を導入し、積雲対流パラメタリゼーションを用いずにLeisnerの雲微物理モデルのみを使用した水平解像度5.5 kmおよび2.26 km鉛直32層の72時間全球大気シミュレーションを行い、衛星データとの比較により、妥当な結果が得られることを確認した。また、上記全球大気コードを用いて、2003年から2004年に日本に上陸した台風に対して、台風進路と強度の72時間(3日間)予測シミュレーションを行い観測結果と比較した結果、進路、強度とも精度よい予測結果が得られることを示した。さらに、本年度導入したネステイング手法を用いて、上記解像度における全球大気シミュレーション後、日本領域を水平1.15 km鉛直に解像し、日本領域の境界に全球シミュレーションより得られたデータを境界条件として与えることで、より詳細な予測を試みた。その結果、特に強度(降雨の強さ、最大風速)予測において結果が改善されうることを確認した。夏季のみではなく、冬季の日本領域における寒気の吹き出しについても再現実験を行い、他のモデルと比較しても遜色のない結果が得られることを示した。

海洋コンポーネントは、水平11 kmの解像度で北太平洋の気候値、平均場を再現する15年シミュレーションに加えて、東海・関東沿岸領域の海流の季節進行を再現する2.25 kmの水平解像度で1年間のシミュレーションを行い、妥当な結果が得られることを確認した。東京湾内や沿岸領域における冬季の北風による湧昇流の再現や、黒潮の北上とともに、沿岸域、湾内の流れ場が影響を受ける様子を再現することができた。今後、海洋観測データとの比較検証も行う予定である。

今後は、本プロジェクト開発した非静力学・大気海洋結合モデルを用いて、より長期にわたる検証実験と予測実験を行い、本結合モデルの有効性ととともに、大気海洋相互作用を

考慮した高解像度予測シミュレーションのインパクトを解析する予定である。加えて、より高精度な数値計算スキーム、およびAMRやCIP法に代表される先進的なスキームを全球、領域モデルに導入するとともに、高速化を含む計算性能についても性能追求を行う。

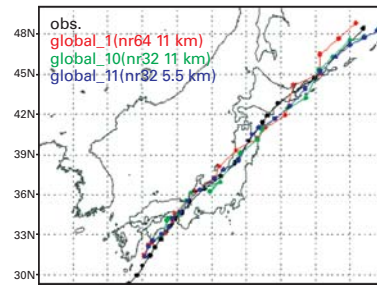


Fig. 1 2003年台風10号(ETAU)の72時間進路予測シミュレーション

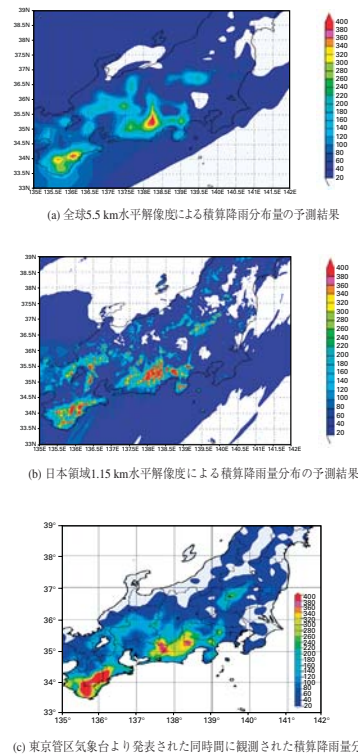


Fig. 2 2003年8月7日0900 UTC から9日0300UTCまでの積算降雨量分布